C. S. Fraser*
Department of Civil Engineering
University of Washington
Seattle, WA 98195

Multiple Focal Setting Self-Calibration of Close-Range Metric Cameras

The technique accommodates the geometric constraint that, at finite focus, symmetrical radial lens distortion varies linearly with magnification.

Introduction

The application of analytical self-calibration methods in close-range photogrammetric surveys involving moderately large photographic scales is accompanied by the requirement to account for variations in lens distortion with changing focussed object distance. Since radial distortion is typically calibrated at infinity focus, the employment of finite focal settings gives rise to the need for further radial distortion functions appropriate to each focal setting. The apparent implication is that, if one employed multiple focal settings in a survey, then multiple camera calibrations would be required. Fortunately, this is not the case. Magill (1955) has shown that the symmetric lens distortion changes linearly with variations in magnification. Based on an extension of Magill's work, Brown (1971) developed a formula relating the radial lens distortion function at any principal distance to the distortion functions at two focal settings, one being typically the infinity focus. Thus, a complete camera calibration need only be carried out for two focal settings to account for the variations in the radial distortion.

Abstract: *Any application of fully analytical techniques in precise close-range photogrammetric surveys involving large photographic scales and varying magnification between individual recorded images must account for variations in lens distortion with changing focussed object distance. In this paper, a multiple focal setting self-calibration technique is developed which accommodates the geometric constraint that, at finite focus, symmetrical radial lens distortion varies linearly with magnification. The required introduction of appropriate linear constraint equations into the normal equation system of the self-calibrating bundle adjustment is outlined. Also, algorithmic aspects of the technique are discussed, especially in relation to the triangular decomposition of the resulting symmetric indefinite "bordered" normal equation matrix. An experiment conducted to assess the practicability of the proposed multiple focal setting self-calibration technique is reported, and the results obtained are discussed.*

In the extension of the self-calibrating bundle adjustment to accommodate multiple cameras or multiple focal settings, the construction of the additional parameter matrix is such that the parameters of the inner cone relating solely to a particular camera or magnification are linearly independent (see, for example, Fraser and Veress, 1979). However, the formula of Brown (1971) expresses a linear dependence between the radial distortion functions at different focussed object distances and the conditions expressed in his formula must be satisfied in a multiple focal setting self-calibration solution for the distortion coefficients at each magnification. Thus, if three or more finite focal settings are employed in a photogrammetric self-calibration, the adopted mathematical model will need to accommodate the inclu-

* Now with the Department of Civil Engineering, University of Canterbury, Christchurch 1, New Zealand.

Photogrammetric Engineering and Remote Sensing,
Vol. 46, No. 9, September 1980, pp. 1161-1171.

sion of linear constraint equations enforcing the relationship between radial lens distortion variations and changes in finite focus.

In this paper, a multiple focal setting self-calibration technique is introduced, in which the normal equation system incorporates appropriate linear constraint equations enforcing a functional dependence between the coefficients of symmetric lens distortion at different magnifications. For the present theoretical development, the case of three focal settings is detailed.

Theoretical Background

Mathematical Model of Self-Calibration

The linearized form of the mathematical model of the self-calibrating bundle method of phototriangulation is given by the matrix equation

$$\begin{bmatrix} \boldsymbol{V} \\ \dot{\boldsymbol{V}} \\ \ddot{\boldsymbol{V}} \\ \dddot{\boldsymbol{V}} \end{bmatrix} + \begin{bmatrix} \dot{\boldsymbol{B}} & \ddot{\boldsymbol{B}} & \dddot{\boldsymbol{B}} \\ -\boldsymbol{I} & 0 & 0 \\ 0 & -\boldsymbol{I} & 0 \\ 0 & 0 & -\boldsymbol{I} \end{bmatrix} \begin{bmatrix} \dot{\boldsymbol{\delta}} \\ \ddot{\boldsymbol{\delta}} \\ \dddot{\boldsymbol{\delta}} \end{bmatrix} = \begin{bmatrix} \boldsymbol{e} \\ \dot{\boldsymbol{e}} \\ \ddot{\boldsymbol{e}} \\ \dddot{\boldsymbol{e}} \end{bmatrix} \tag{1}$$

where

$\dot{\boldsymbol{\delta}}, \ddot{\boldsymbol{\delta}}, \dddot{\boldsymbol{\delta}}$ represent the vectors of corrections to the exterior orientation elements, the object space coordinates, and the additional parameters which comprise the systematic image error correction model;

$\dot{\boldsymbol{B}}, \ddot{\boldsymbol{B}}, \dddot{\boldsymbol{B}}$ refer to the matrices of partial derivatives of the extended collinearity equations with respect to the exterior orientation elements, the object space coordinates, and the additional parameters;

$\boldsymbol{V}, \dot{\boldsymbol{V}}, \ddot{\boldsymbol{V}}, \dddot{\boldsymbol{V}}$ are the vectors of residuals for the image point coordinates, the exterior orientation elements, the object space coordinates, and the additional parameters;

$\boldsymbol{e}, \dot{\boldsymbol{e}}, \ddot{\boldsymbol{e}}, \dddot{\boldsymbol{e}}$ indicate the discrepancy vectors; and

$\boldsymbol{I}$ is the unit matrix.

In the form given by Equation 1, all parameters are treated as observed or pseudo-observed quantities of known *a priori* reliability. The block-diagonal weight matrix, $\boldsymbol{P}$, expressing *a priori* precision is given as

$$\boldsymbol{P} = \begin{bmatrix} \boldsymbol{W} & & & \\ & \dot{\boldsymbol{W}} & & \\ & & \ddot{\boldsymbol{W}} & \\ & & & \dddot{\boldsymbol{W}} \end{bmatrix}$$

where $\boldsymbol{W}, \dot{\boldsymbol{W}}, \ddot{\boldsymbol{W}}, \dddot{\boldsymbol{W}}$ are the weight matrices of the image coordinates, the elements of exterior orientation, the object space coordinates, and the additional parameters.

The normal equations for a linear least-squares solution of the parametric system, Equation 1, assume the form

$$\begin{bmatrix} \dot{\boldsymbol{B}}^{\mathrm{T}}\boldsymbol{W}\dot{\boldsymbol{B}} + \dot{\boldsymbol{W}} & \dot{\boldsymbol{B}}^{\mathrm{T}}\boldsymbol{W}\ddot{\boldsymbol{B}} & \dot{\boldsymbol{B}}^{\mathrm{T}}\boldsymbol{W}\dddot{\boldsymbol{B}} \\ & \ddot{\boldsymbol{B}}^{\mathrm{T}}\boldsymbol{W}\ddot{\boldsymbol{B}} + \ddot{\boldsymbol{W}} & \ddot{\boldsymbol{B}}^{\mathrm{T}}\boldsymbol{W}\dddot{\boldsymbol{B}} \\ \text{symmetric} & & \dddot{\boldsymbol{B}}^{\mathrm{T}}\boldsymbol{W}\dddot{\boldsymbol{B}} + \dddot{\boldsymbol{W}} \end{bmatrix} \begin{bmatrix} \dot{\boldsymbol{\delta}} \\ \ddot{\boldsymbol{\delta}} \\ \dddot{\boldsymbol{\delta}} \end{bmatrix} = \begin{bmatrix} \dot{\boldsymbol{B}}^{\mathrm{T}}\boldsymbol{W}\boldsymbol{e} - \dot{\boldsymbol{W}}\dot{\boldsymbol{e}} \\ \ddot{\boldsymbol{B}}^{\mathrm{T}}\boldsymbol{W}\boldsymbol{e} - \ddot{\boldsymbol{W}}\ddot{\boldsymbol{e}} \\ \dddot{\boldsymbol{B}}^{\mathrm{T}}\boldsymbol{W}\boldsymbol{e} - \dddot{\boldsymbol{W}}\dddot{\boldsymbol{e}} \end{bmatrix} \tag{2}$$

Equation 2 represents the general system of normal equations for the self-calibrating bundle adjustment of a photogrammetric block generated by any combination of image coordinate measurements and parameters of the exterior orientation, the object space reference system, and the image correction model. For a comprehensive review of the fine structure of portions of Equation 2, the reader is referred to Brown (1976).

Additional Parameters

The additional parameters, $\dddot{\boldsymbol{\delta}}$, with coefficient matrix, $\dddot{\boldsymbol{B}}$, describe the correction model for systematic image coordinate errors. In expanded form, the model adopted for the present application is given by the following equations, in which Δx and Δy indicate the image coordinate corrections:

$$\begin{aligned} \Delta x &= \Delta x_F + \Delta x_B \\ \Delta y &= \Delta y_F + \Delta y_B \end{aligned} \tag{3}$$

Here, Δx_F and Δy_F contain correction terms which relate to a specific Gaussian focal length or principal distance c_i:

$$\begin{aligned}\Delta x_F &= x(K_{i1}r^2 + K_{i2}r^4 + K_{i3}r^6) + P_{i1}(3x^2 + y^2) + 2P_{i2}xy + (-x/c_i)dc_i \\ \Delta y_F &= y(K_{i1}r^2 + K_{i2}r^4 + K_{i3}r^6) + 2P_{i1}xy + P_{i2}(x^2 + 3y^2) + (-y/c_i)dc_i\end{aligned} \tag{4}$$

where

$$\begin{aligned}x &= x' - x_0 \\ y &= y' - y_0 \\ r &= (x^2 + y^2)^{1/2}\end{aligned}$$

and

x',y'	are the observed image coordinates;
x_0,y_0	are the coordinates of the principal point;
c_i	is the Gaussian focal length, or principal distance;
dc_i	is the correction to c_i;
K_{i1},K_{i2},K_{i3}	are the coefficients of symmetric radial lens distortion (see Equation 6); and
P_{i1},P_{i2}	are the decentering distortion coefficients.

In the following discussion, the additional parameters which relate to a specific principal distance, namely $K_{i1},K_{i2},K_{i3},P_{i1},P_{i2}$, and dc_i, will be referred to as focal setting-invariant parameters.

The expressions for the image coordinate corrections Δx_B and Δy_B comprise terms which are treated as block-invariant in nature:

$$\begin{aligned}\Delta x_B &= -x_0 + a_1xy + a_2y^2 + a_3x^2y + a_4xy^2 \\ \Delta y_B &= -y_0 + b_1x + b_2y + b_3xy + b_4x^2 + b_5x^2y + b_6xy^2\end{aligned} \tag{5}$$

Consideration of the interior orientation parameters x_0 and y_0 as block-invariant is based on the assumption that the camera is free of significant lens barrel misalignment. Of the remaining block-invariant parameters, a_1 through a_4 and b_1 through b_6, the linear terms in x and y account for a lack of orthogonality and a differential scale component between the image coordinate axes. Schut (1978) has reported that it is immaterial whether the two linear terms are used to correct x, y, or both. The larger depth of spacing typically encountered in close-range object target arrays makes it appropriate to retain the terms a_1xy and b_3xy rather than the two omitted second-order terms in x^2 and y^2. Gotthardt (1975) has presented an illustration of the geometric effect of each of the empirical terms in Equations 5, for an image having a standard 3 × 3 point configuration.

Perhaps the distinguishing feature of the image correction model, Equations 3, is that it facilitates the recovery of inner cone parameters of the camera, thus providing a physical insight into the systematic error attributable to radial and decentering distortion, and to biases in the elements of interior orientation. This self-calibration approach has been adopted by a number of investigators (see, for example, Kenefick *et al.*, 1972; Salmenpëra *et al.*, 1974; Brown, 1974; Brown, 1976). Alternative formulations of the image correction model which incorporate orthogonal polynomials (Ebner, 1976; Grün, 1978) or harmonic functions (El Hakim and Faig, 1979) may be viewed as providing systematic error compensation without giving any precise indication of the nature of the individual error sources.

VARIATION IN LENS DISTORTION WITH CHANGING FOCAL SETTING

Based on the original formulation of Magill (1955) and the subsequent developments by Brown (1971), Abdel-Aziz (1973) has derived the following formulae for the description of symmetric radial lens distortion at three different focal settings:

$$\begin{aligned}\Delta r_{c1} &= K_{11}r^3 + K_{12}r^5 + K_{13}r^7 + \ldots \\ \Delta r_{c2} &= K_{21}r^3 + K_{22}r^5 + K_{23}r^7 + \ldots \\ \Delta r_{c3} &= K_{31}r^3 + K_{32}r^5 + K_{33}r^7 + \ldots\end{aligned} \tag{6}$$

and

$$\begin{aligned}K_{31} &= \alpha\left[\frac{c_1}{c_3}\right]^3 K_{11} + (1 - \alpha)\left[\frac{c_2}{c_3}\right]^3 K_{21} \\ K_{32} &= \alpha\left[\frac{c_1}{c_3}\right]^5 K_{12} + (1 - \alpha)\left[\frac{c_2}{c_3}\right]^5 K_{22} \\ K_{33} &= \alpha\left[\frac{c_1}{c_3}\right]^7 K_{13} + (1 - \alpha)\left[\frac{c_2}{c_3}\right]^7 K_{23}\end{aligned} \tag{7}$$

where

$$\alpha = \frac{c_3 - c_2}{c_1 - c_2} \tag{8}$$

Here, Δr_{c1} and Δr_{c2} are the radial distortion functions for principal distances c_1 and c_2, whereas Δr_{c3} is the unknown distortion at any other principal distance c_3. The expression for α can also be given in terms of the focal length of the lens, f, and the focussed object distance, s_i; Brown (1972) has given Equation 8 in the form

$$\alpha = \frac{s_2 - s_3}{s_2 - s_1} \cdot \frac{s_1 - f}{s_3 - f}$$

By referring to the standard thin lens equation

$$\frac{1}{s_i} + \frac{1}{c_i} = \frac{1}{f} \tag{9}$$

the equivalence of the two expressions for the variable, α, can be readily shown. In the context of applying constraint equations enforcing the linear relationship between the coefficients of the three distortion functions, it is preferable to recast Equations 7 into the form

$$\begin{aligned}
&(c_3 - c_2)\, c_1^3 K_{11} + (c_1 - c_3)\, c_2^3 K_{21} + (c_2 - c_1)\, c_3^3 K_{31} = 0 \\
&(c_3 - c_2)\, c_1^5 K_{12} + (c_1 - c_3)\, c_2^5 K_{22} + (c_2 - c_1)\, c_3^5 K_{32} = 0 \\
&(c_3 - c_2)\, c_1^7 K_{13} + (c_1 - c_3)\, c_2^7 K_{23} + (c_2 - c_1)\, c_3^7 K_{33} = 0
\end{aligned} \tag{10}$$

Although Equations 10 represent linear condition equations in terms of the coefficients K_{i1}, K_{i2}, and K_{i3}, the expressions are non-linear with respect to the principal distances c_1, c_2, and c_3. The introduction of approximate values for the parameters, and linearization by Taylor series expansion yields for the r^3 term of the distortion polynomial

$$\begin{aligned}
&(c_3 - c_2)c_1^3 dK_{11} + (c_1 - c_3)c_2^3 dK_{21} + (c_2 - c_1)c_3^3 dK_{31} \\
&+ \left[3c_1^2(c_3 - c_2)K_{11} + (1 - c_3)c_2^3 K_{21} + (c_2 - 1)c_3^3 K_{31}\right] dc_1 \\
&+ \left[(c_3 - 1)c_1^3 K_{11} + 3c_2^2(c_1 - c_3)K_{21} + (1 - c_1)c_3^3 K_{31}\right] dc_2 \\
&+ \left[(1 - c_2)c_1^3 K_{11} + (c_1 - 1)c_2^3 K_{21} + 3c_3^2(c_2 - c_1)K_{31}\right] dc_3 \\
&+ \left[(c_3 - c_2)c_1^3 K_{11} + (c_1 - c_3)c_2^3 K_{21} + (c_2 - c_1)c_3^3 K_{31}\right] = 0
\end{aligned} \tag{11}$$

where dK_{i1}, dK_{i2}, dK_{i3} are corrections to current values of the radial lens distortion coefficients.

Similar expressions can be derived for the fifth and seventh order terms of the radial distortion function; however, only the condition equation for the term in r^5 is included here as the coefficients, K_{i3}, were at no time statistically significant in the practical self-calibrations conducted. The linearization of the expression relating the coefficients, K_{i2}, is given by

$$\begin{aligned}
&(c_3 - c_2)c_1^5 dK_{12} + (c_1 - c_3)c_2^5 dK_{22} + (c_2 - c_1)c_3^5 dK_{32} \\
&+ \left[5c_1^4(c_3 - c_2)K_{12} + (1 - c_3)c_2^5 K_{22} + (c_2 - 1)c_3^5 K_{32}\right] dc_1 \\
&+ \left[(c_3 - 1)c_1^5 K_{12} + 5c_2^4(c_1 - c_3)K_{22} + (1 - c_1)c_3^5 K_{32}\right] dc_2 \\
&+ \left[(1 - c_2)c_1^5 K_{12} + (c_1 - 1)c_2^5 K_{22} + (c_2 - c_1)5c_3^4 K_{32}\right] dc_3 \\
&+ \left[(c_3 - c_2)c_1^5 K_{12} + (c_1 - c_3)c_2^5 K_{22} + (c_2 - c_1)c_3^5 K_{32}\right] = 0
\end{aligned} \tag{12}$$

In matrix notation, Equations 11 and 12 can be written as a combined expression:

$$\boldsymbol{H}\ddot{\boldsymbol{\delta}}_h + \boldsymbol{F} = 0 \tag{13}$$

For a multiple focal setting self-calibration employing three finite object distances, neglecting the seventh-order terms of the distortion polynomials, Equation 13 can be given in the expanded form

$$\left[\begin{array}{ccc:ccc:ccc}
h_{11} & 0 & h_{13} & h_{14} & 0 & h_{16} & h_{17} & 0 & h_{19} \\
0 & h_{22} & h_{23} & 0 & h_{25} & h_{26} & 0 & h_{28} & h_{29}
\end{array}\right]
\left[\begin{array}{c}
dK_{11} \\ dK_{12} \\ dc_1 \\ \hdashline dK_{21} \\ dK_{22} \\ dc_2 \\ \hdashline dK_{31} \\ dK_{32} \\ dc_3
\end{array}\right]
+ \left[\begin{array}{c} f_1 \\ \hdashline f_2 \end{array}\right] = 0 \tag{14}$$

INCORPORATION OF DISTORTION COEFFICIENT CONSTRAINT EQUATIONS

The linearized equations, Equations 11 and 12, represent geometric conditions between the radial lens distortion coefficients, K_{ij}, which are themselves unknown parameters to be solved for in the self-calibration adjustment. The appropriate observation equation form in cases where there is a functional dependence between the parameters of the mathematical model, can be given by the parametric system

$$\begin{aligned} -\mathbf{V} + \mathbf{A}\mathbf{X} - \mathbf{L} &= 0; \mathbf{P} \\ \mathbf{H}\ddot{\boldsymbol{\delta}}_h + \mathbf{F} &= 0 \end{aligned} \tag{15}$$

where $\mathbf{A}$ is the design matrix, $\mathbf{X}$ the vector of u unknown parameters ($\mathbf{X}^T = [\dot{\boldsymbol{\delta}}^T \ddot{\boldsymbol{\delta}}^T \dddot{\boldsymbol{\delta}}^T]$), $\mathbf{L}$ the discrepancy vector, $\mathbf{V}$ the vector of residuals, and $\mathbf{P}$ the weight matrix.

With the incorporation of k linear constraint equations, the following system of normal equations is formed, noting that the parameters $\dddot{\boldsymbol{\delta}}_h$ are contained in $\mathbf{X}$:

$$\begin{bmatrix} \mathbf{A}^T\mathbf{P}\mathbf{A} & \mathbf{H}^T \\ \mathbf{H} & 0 \end{bmatrix} \begin{bmatrix} \mathbf{X} \\ -\mathbf{K}_c \end{bmatrix} - \begin{bmatrix} \mathbf{A}^T\mathbf{P}\mathbf{L} \\ -\mathbf{F} \end{bmatrix} = 0 \tag{16}$$

This system is square, representing $(u + k)$ equations in $(u + k)$ unknowns. With the inclusion of the unknowns $\mathbf{K}_c$, which are the individual lagrangian multipliers or correlates, the number of degrees of freedom in the adjustment is incremented by k. From Equation 16, it is apparent that the usual normal equation matrix $\mathbf{A}^T\mathbf{P}\mathbf{A}$ has been "bordered" by the equations expressing the functional dependence between the parameters. The original derivation of this method is attributed to the German geodesist and mathematician, Helmert.

The bordered normal equations of the photogrammetric self-calibrating bundle adjustment, incorporating geometric conditions between additional parameters, follow from a substitution of the matrices in Equation 2 into Equation 16:

$$\begin{bmatrix} \dot{\mathbf{B}}^T\mathbf{W}\dot{\mathbf{B}} + \dot{\mathbf{W}} & \dot{\mathbf{B}}^T\mathbf{W}\ddot{\mathbf{B}} & \dot{\mathbf{B}}^T\mathbf{W}\dddot{\mathbf{B}} & 0 \\ & \ddot{\mathbf{B}}^T\mathbf{W}\ddot{\mathbf{B}} + \ddot{\mathbf{W}} & \ddot{\mathbf{B}}^T\mathbf{W}\dddot{\mathbf{B}} & 0 \\ & & \dddot{\mathbf{B}}^T\mathbf{W}\dddot{\mathbf{B}} + \dddot{\mathbf{W}} & \mathbf{H}^T \\ \text{symmetric} & & & 0 \end{bmatrix} \begin{bmatrix} \dot{\boldsymbol{\delta}} \\ \ddot{\boldsymbol{\delta}} \\ \dddot{\boldsymbol{\delta}} \\ -\mathbf{K}_c \end{bmatrix} = \begin{bmatrix} \dot{\mathbf{B}}^T\mathbf{W}\mathbf{e} - \dot{\mathbf{W}}\dot{\mathbf{e}} \\ \ddot{\mathbf{B}}^T\mathbf{W}\mathbf{e} - \ddot{\mathbf{W}}\ddot{\mathbf{e}} \\ \dddot{\mathbf{B}}^T\mathbf{W}\mathbf{e} - \dddot{\mathbf{W}}\dddot{\mathbf{e}} \\ -\mathbf{F} \end{bmatrix} \tag{17}$$

COMPUTATIONAL CONSIDERATIONS

Typically, the rank $(u + k)$ of the bordered normal equation matrix in Equation 17 exceeds that of the usual normal coefficient matrix by only two or three. Therefore, with $k << u$, it is computationally advantageous to consider a direct solution for the bordered system. So long as the mathematical model has been constructed correctly, and assuming that the coefficient matrix is not excessively ill-conditioned, the bordered matrix will lend itself to inversion by standard techniques.

In the present investigation, a Cholesky factorization utilizing symmetric storage mode has been employed as the solution algorithm of the normal equations, Equations 2, for the self-calibrating bundle adjustment. However, such an algorithm cannot be used for the solution of the bordered system. The Cholesky factorization involves a decomposition of a matrix, $\mathbf{N}$, into the form $\mathbf{L}\mathbf{L}^T$, where $\mathbf{L}$ is a lower triangular matrix. The product, $\mathbf{L}\mathbf{L}^T$, is always positive semi-definite, so the decomposition will fail in exact arithmetic unless the matrix, $\mathbf{N}$, is positive-definite. Algorithmically, failure in exact arithmetic is associated with severe instability in finite precision. The introduction of a null principal submatrix of order two in the formation of the bordered normal matrix causes the matrix to become indefinite. Thus, an alternative to the Cholesky factorization must be found.

At first sight Gaussian elimination with partial or complete pivoting may appear to present a useful alternative solution technique. In typical Gauss elimination the matrix, $\mathbf{N}$, is factored into the form, $\mathbf{L}\mathbf{D}\mathbf{L}^T$, where $\mathbf{D}$ is diagnonal. In applying complete pivoting, the first trailing submatrix produced will generally no longer be symmetric. However, it is both advantageous and economical to employ a symmetric storage mode and, thus, a factorization which maintains symmetry is preferred. To preserve this symmetry, the choice of pivots is restricted to the diagonal elements as the interchange of two rows must be accompanied by the interchange of the same two columns. But the bordered matrix has a null principal submatrix which will give rise to zero pivots.

A block Gaussian elimination technique which takes advantage of the symmetry of an indefinite matrix and circumvents the problem of zero pivots has been developed by Bunch and Parlett (1971). The scheme involves a decomposition of the matrix, $\mathbf{N}$, to $\mathbf{M}\mathbf{D}\mathbf{M}^T$, where $\mathbf{D}$ is a symmetric block diagonal matrix and $\mathbf{M}$ is a unit lower triangular matrix. Each block of $\mathbf{D}$ is of the order 1 or 2, and $\mathbf{M}_{i+1,i} = 0$ whenever $\mathbf{D}_{i+1,i} \neq 0$. The algorithm for this factorization is faster than Gauss elimination and almost as

stable as Gauss elimination with complete pivoting. For the solution of the bordered normal equation system, Equation 17, such an algorithm has been used.

In addition to the requirement for a direct solution of the parameters $\dot{\boldsymbol{\delta}}$, $\ddot{\boldsymbol{\delta}}$, and $\dddot{\boldsymbol{\delta}}$ (K_c is typically not required), the cofactor matrix, $\boldsymbol{Q}_{xx}$, is needed in order to carry out an evaluation of the *a posteriori* precision of the parameters. It can be shown that $\boldsymbol{Q}_{xx}$ is equal to the leading principal submatrix of the inverse of the bordered normal equation matrix. That is, from Equation 16

$$\begin{bmatrix} \boldsymbol{A}^{\mathrm{T}}\boldsymbol{P}\boldsymbol{A} & \boldsymbol{H}^{\mathrm{T}} \\ \boldsymbol{H} & 0 \end{bmatrix}^{-1} = \begin{bmatrix} \boldsymbol{Q}_{xx} & \boldsymbol{\beta}^{\mathrm{T}} \\ \boldsymbol{\beta} & \boldsymbol{\gamma} \end{bmatrix} \tag{18}$$

A direct inversion of the bordered normal equation matrix will therefore yield cofactor matrices, $\boldsymbol{Q}_{\dot{\delta}\dot{\delta}}$, for the elements of exterior orientation, $\boldsymbol{Q}_{\ddot{\delta}\ddot{\delta}}$ for the object point coordinates, and $\boldsymbol{Q}_{\dddot{\delta}\dddot{\delta}}$ for the additional parameters:

$$\boldsymbol{Q}_{xx} = \begin{bmatrix} \boldsymbol{Q}_{\dot{\delta}\dot{\delta}} & \boldsymbol{Q}_{\dot{\delta}\ddot{\delta}} & \boldsymbol{Q}_{\dot{\delta}\dddot{\delta}} \\ & \boldsymbol{Q}_{\ddot{\delta}\ddot{\delta}} & \boldsymbol{Q}_{\ddot{\delta}\dddot{\delta}} \\ \text{symmetric} & & \boldsymbol{Q}_{\dddot{\delta}\dddot{\delta}} \end{bmatrix} \tag{19}$$

From the theoretical and computational aspects presented in the foregoing discussion, a practical multiple focal setting self-calibration method can be developed.

Experimental Verification

Details of the Experiment

In order to verify the proposed simultaneous multiple focal setting self-calibration technique and also to assess its practicability, an experiment was conducted. In the following paragraphs details of the experiment relating to the photographic procedure, the camera used, the geometry of the system, and the initial data processing are presented.

The Camera. The camera selected for the experiment was an MK-70 metric Hasselblad (serial no. 1146) with a Biogon 60mm *f*/5.6 lens. While a film camera with a wide angle lens does not represent the most desirable system for a conclusive experimental verification of the proposed self-calibration technique, it does display a few practical advantages. In the case of the Hasselblad, the incorporation of a reseau grid contributes to a minimizing of the effects of film deformation, although residual deformation components of 3-4 μm seem to persist regardless of the adopted image transformation and subsequent analytical phototriangulation technique.

For a successful recovery of the Gaussian focal length, convergent photography and a well distributed three-dimensional object target field are typically required. The large depth of field obtained using a 60mm lens at *f*-stop 32 makes it possible to employ highly convergent camera axes and a large depth of spacing in the target field. In the present experiment the extreme case was reached where at a focal setting of 1.6 m, the range of the acceptable photographic distance within the field of view, was from 1 m to 2.7 m. At f-stop 32 all targets appeared in focus and the variation of distortion throughout the photographic field, obtained using the formulae derived by Brown (1971; 1972), was a maximum of 5 percent and typically less than 0.5 μm.

Geometry of the System. The configuration of the exposure stations and the geometry of the object target field are illustrated in Figure 1. The three-dimensional target range partly comprised a planar field, namely a wall, consisting of 29 points, each target point being the 4-mm diameter spherical head of a map tack. In addition, two piano wires were suspended as plumb lines 36 cm out from the wall at a separation of 60 cm, symmetric about the center of the target field. On each of the wires six 3-mm diameter seed-beads were fixed to serve as targets. The approximate overall dimensions of the target range were 2.6 m wide, 2.3 m high, and 0.4 m deep.

As illustrated in Figure 1, 12 camera stations were employed, four corresponding to each of the three adopted focal settings, of 3 m, 2 m, and 1.6 m. All camera axes were directed toward the center point of the target field, which at the 3 m range gives rise to phi rotations of magnitude approximately 45° at exposure stations 1 and 2 (angle of convergence of 90°). At these same exposure stations the cameras were inclined with an omega rotation of 6°, while at camera station 4 the omega rotation was −12°. At station 3 the camera axis was approximately normal to the *XY* plane. By simply scaling down the exposure station configuration at 3 m in proportion to focal setting, similar camera configurations were set up at object distances of 2 m and 1.6 m.

A large divergency of swing angles was incorporated to enhance the precise recovery of interior orientation elements x_0 and y_0. The kappa rotation at any of the four camera stations for a particular focal setting was either 90° or 180° different from the value at the remaining three stations.

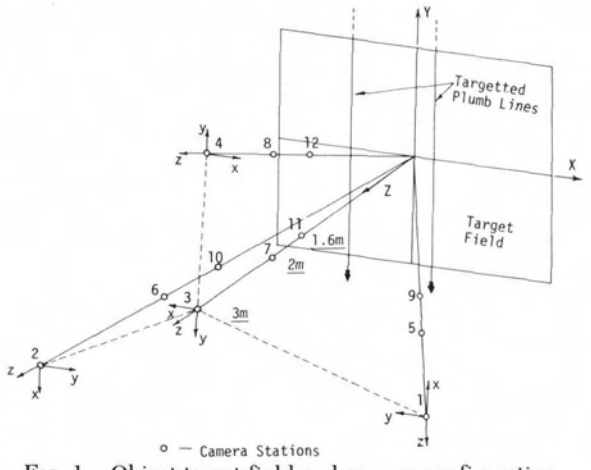

FIG. 1. Object target field and camera configuration.

Object target point density was such that, on the average, 25 image points appeared on the photographs taken at the 1.6-m focus, whereas the number of points imaged at 2-m and 3-m focal settings averaged 30 and 39, respectively. Of the 41 object points in the target field, all but three appeared on at least four photographs. On each exposure, points were well distributed throughout the image format with their layout affording a wide distribution of radial distance.

Photographic Procedure. All 12 photographs were exposed over a 1-hour period on the same role of 70 mm film. Each exposure time was ½ sec. at *f*-stop 32. Only three focal settings were used: 3 m for exposure stations 1, 2, 3, and 4; 2 m for stations 5, 6, 7, and 8; and 1.6 m for stations 9, 10, 11, and 12.

Data Reduction. Image coordinate observations were carried out on an OMI-Bendix AP/C analytical stereoplotter, with each negative being viewed monocularly. In addition to measuring the x,y coordinates of all points which were clearly definable, the coordinates of eight reseau crosses were observed.

The computations presented in this paper were carried out using two main computer programs, SELCAL and MULFOC. The former is a self-calibrating bundle adjustment specifically written for close-range applications, the latter is a modified version of SELCAL, which incorporates the bordering of the normal equations by the linear constraint equations, Equations 14.

SELF-CALIBRATION ADJUSTMENTS

It is possible to carry out multiple focal setting self-calibration adjustments either with or without the inclusion of the constraint equations enforcing a linear variation in radial lens distortion with changing principal distance. Where the constraint equations are not applied, there is no correlation between the lens distortion parameters at the different focal settings, and the adjustment becomes a special case of the multiple camera self-calibration (see, for example, Fraser and Veress, 1979). A distinguishing feature, however, is that, unlike the multiple camera case, it is possible to carry the interior orientation elements x_0 and y_0 as block-invariant parameters in the adjustment.

The bordering of the normal equations of the bundle adjustment with constraint equations can give rise to a few practical problems. It was found that the decomposition of the symmetric indefinite bordered system was unstable in situations where the additional parameter set included terms which were not statistically significant. For this reason the self-calibration adjustment with constraints was only carried out after a number of SELCAL runs were made. This enabled the determination of the most appropriate focal setting-invariant and block-invariant parameter sets and also enabled the suppression of additional parameters which were not statistically significant.

Having determined the most appropriate terms for the correction model, the self-calibration with linear constraints could be carried out. The inclusion of the same inner cone and film deformation parameters in the MULFOC runs then facilitated a direct comparison of the results with those obtained using the self-calibration program SELCAL.

ADJUSTMENTS WITHOUT LINEAR CONSTRAINTS

IMAGE CORRECTION MODEL

Of a number of additional parameter sets chosen for individual runs of SELCAL, the correction model which produced the most favorable results from the point of view of statistical significance and the minimization of the mean square estimate of image coordinate residuals was as follows:

$$\Delta x_F = xr^2K_{i1} + xr^4K_{i2} + (-x/c_i)dc_i + (3x^2 + y^2)P_{i1} + 2xyP_{i2}$$
$$\Delta y_F = yr^2K_{i1} + yr^4K_{i2} + (-y/c_i)dc_i + 2xyP_{i1} + (x^2 + 3y^2)P_{i2} \quad (20)$$

and

$$\Delta x_B = -x_0 + a_4xy^2$$
$$\Delta y_B = -y_0 + b_1x + b_5x^2y + b_6xy^2 \quad (21)$$

Initial adjustments were carried out in which the coordinates, x_0 and y_0, of the principal point were incorporaatd as focal setting-invariant parameters. However, the calculated values at each magnification differed by significantly less than the one sigma level. In the absence of any distinguishable lens barrel misalignment, the two interior orientation parameters were then assumed to be block-invariant. In treating x_0 and y_0 as block-invariant, the strong correlation between these parameters and the coefficients of decentering distortion, P_{i1} and P_{i2}, at each focus is considerably reduced. Typically, the values of the correlation coefficients dropped from about 0.9 to about 0.65. Such a reduction in the extent of linear dependence between parameters can only enhance solution stability.

The statistical significance of the block-invariant additional parameters was verified by examining the null hypothesis that the derived estimates were equal to zero. Since there is little correlation between the individual parameters, a hypothesis H_0 of rank $(H_0) = 1$ was selected, the chosen significance level being 5 percent (confidence level of 95 percent). For all six block-invariant additional parameters, the null hypothesis had to be rejected.

Perhaps the most notable feature of the derived optimum block-invariant additional parameter set is the lack of significant second-order terms. The absence of terms in xy, x^2, and y^2 indicates that to a large degree the linearized projective equations used for the initial two-dimensional image coordinate transformations accounted for the second-order film deformation. However, higher order residual deformation remained and a small first-order component was introduced.

Of the focal setting-invariant parameters, the dominant term of the decentering distortion function was found to be significant at all three principal distances and the derived decentering profile displayed a systematic variation with changing focal setting. The variation was, however, by no means linear and can perhaps be attributed to a slight misalignment between the axis of the focusing barrel and the axis of the lens (see Brown, 1971; 1972). Variations in the decentering phase angle were consistent with the measured angles of rotation of the lens barrel between the three focal settings.

RADIAL DISTORTION AND GAUSSIAN FOCAL LENGTH

The derived least-squares estimates for the radial distortion coefficients, K_{i1} and K_{i2}, and for the Gaussian focal length at each of the three focal settings are listed in Table 1. Also shown in the table are the *a posteriori* standard errors of these parameters. For each focal setting the following *a priori* precisions

TABLE 1. LEAST-SQUARES ESTIMATES AND STANDARD ERRORS OF RADIAL LENS DISTORTION COEFFICIENTS AND GAUSSIAN FOCAL LENGTHS

	Unconstrained		Constrained	
Parameter	Estimate $\hat{x}$	Std. Error $\hat{\sigma}_x$	Estimate $\hat{x}$	Std. Error $\hat{\sigma}_x$
1.6m				
c_1 (mm)	63.840	0.015	63.848	0.015
K_{11} (mm^{-2})	−0.188E-5	0.51E-6	−0.130E-5	0.46E-6
K_{12} (mm^{-4})	0.103E-8	0.44E-9	0.652E-9	0.38E-9
		($\rho K_{11}K_{12} = -0.95$)**		($\rho K_{11}K_{12} = -0.95$)
2m				
c_2	63.303	0.016	63.284	0.014
K_{21}	−0.247E-6	0.43E-6	−0.796E-6	0.33E-6
K_{22}	−0.858E-10	0.35E-9	0.279E-9	0.24E-9
		($\rho K_{21}K_{22} = -0.96$)		($\rho K_{21}K_{22} = -0.88$)
3m				
c_3	62.560	0.018	62.559	0.017
K_{31}	−0.435E-6	0.45E-6	−0.103E-6	0.42E-6
K_{32}	−0.258E-9	0.30E-9	−0.252E-9	0.29E-9
		($\rho K_{31}K_{32} = -0.85$)		($\rho K_{31}K_{32} = -0.84$)

** Correlation Coefficient.

were assigned: $\sigma_{c_i} = \pm 0.1$ mm, $\sigma_{K_{i1}} = \pm 0.5$E-5 and $\sigma_{K_{i2}} = \pm 0.5$E-8. Plots of the radial distortion curves obtained in the adjustment are presented in Figure 2, along with the one sigma limit of the distortion polynomial relating to the 2-m focal setting.

A comparison of the radial distortion polynomials obtained in the unconstrained adjustment with those obtained in the self-calibration with linear constraints will be treated in a following section. However, it is useful at this time to consider the statistical significance of the derived symmetric lens distortion functions, which have the form

$$\Delta r_i = K_{i1} r^3 + K_{i2} r^5 \tag{22}$$

To ascertain the statistical significance of the coefficients K_{i1} and K_{i2}, a null hypothesis H_0 of rank $(H_0) = 2$ is required because of the high correlation between these two parameters (Hamilton, 1964; Grün, 1978). The null hypothesis becomes

$$H_0 : K_{i1} = 0; K_{i2} = 0$$

The statistic $\boldsymbol{T}$ is calculated from the matrix equation

$$\boldsymbol{T} = \tfrac{1}{2}[\hat{K}_{i1}\ \hat{K}_{i2}] \begin{bmatrix} \hat{\sigma}^2_{K_{i1}} & \hat{\sigma}_{K_{i1}K_{i2}} \\ \hat{\sigma}_{K_{i1}K_{i2}} & \hat{\sigma}^2_{K_{i2}} \end{bmatrix}^{-1} \begin{bmatrix} \hat{K}_{i1} \\ \hat{K}_{i2} \end{bmatrix} \tag{23}$$

where $\hat{K}_{i1}, \hat{K}_{i2}$ are the least-squares estimates; and $\hat{\sigma}^2_{K_{i1}}, \hat{\sigma}^2_{K_{i2}}$ are the *a posteriori* variances of the estimates.

The null hypothesis can only be rejected at the 5 percent significance level when $\boldsymbol{T}$ is greater than the Fisher statistic $F_{2,\infty,0.05}$; that is, when

$$\boldsymbol{T} > F_{2,\infty,0.05} = 3.0$$

Application of the above test to the estimates for K_{i1} and K_{i2} at each of the three focal settings yielded the following results: At a confidence level of 95 percent the null hypothesis could be rejected for focal settings of 1.6 m and 3 m. However, the hypothesis could not be rejected for the distortion polynomial at 2 m. Thus, the derived radial distortion function for the 2 m focal setting cannot be regarded as statistically significant at the specified confidence level.

Self-Calibration with Linear Constraints

Image Correction Model

In the multiple focal setting self-calibration adjustment, program MULFOC, the image correction model comprised the same terms as those used for the self-calibration without linear constraints. The adjusted values and *a posteriori* precision of the block-invariant parameters and the decentering distortion coefficients obtained via the program MULFOC were not significantly different from the corresponding estimates determined in the unconstrained adjustment.

Radial Distortion and Gaussian Focal Length

Preliminary testing of the multiple focal setting self-calibration program MULFOC which incorporated the constraint equations, Equation 14, indicated that a satisfactory convergence to the linear conditions

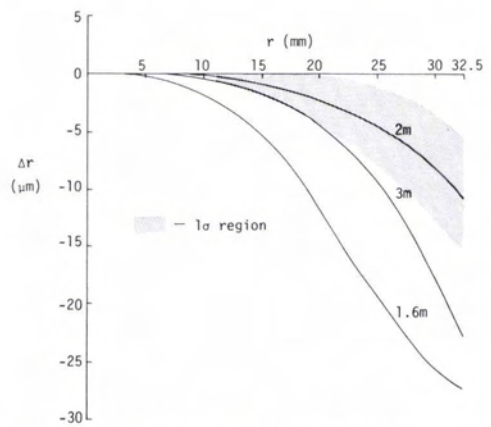

FIG. 2. Symmetric radial lens distortion—unconstrained adjustment.

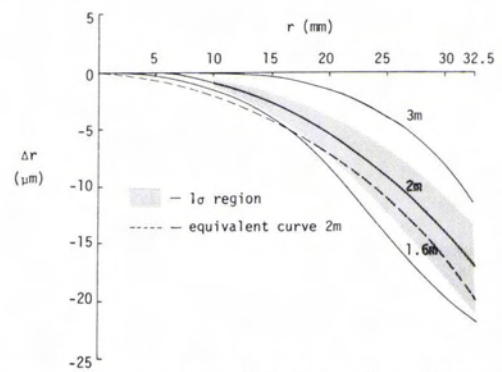

FIG. 3. Symmetric radial lens distortion—constrained adjustment.

was achieved only when the *a priori* estimates for the principal distances, c_i, were given large weights (say, $\sigma_{c_i} \simeq 0.010$ mm). To overcome the lack of satisfactory numerical determinacy of the linearized constraint equations in cases where loose *a priori* weights were assigned to the estimates c_i, the terms in dc_i were suppressed. This arbitrary assignment of selected coefficient values to zero did not effect the final adjustment solution and overcame the convergence problems. Thus, for the following discussion Equation 14 is modified to the form:

$$\left[\begin{array}{cc:cc:cc} h_{11} & 0 & h_{14} & 0 & h_{17} & 0 \\ 0 & h_{22} & 0 & h_{25} & 0 & h_{28} \end{array}\right] \left[\begin{array}{c} dK_{11} \\ dK_{12} \\ \hdashline dK_{21} \\ dK_{22} \\ \hdashline dK_{31} \\ dK_{32} \end{array}\right] + \left[\begin{array}{c} f_1 \\ \hdashline f_2 \end{array}\right] = 0 \tag{20}$$

The incorporation of Equation 20 into the program MULFOC enabled a self-calibration to be carried out in which the assigned *a priori* variances of the additional parameters were of the same value as those used in the SELCAL runs. The adjusted values of the parameters c_i and K_{i1}, K_{i2} obtained in the constrained solution are listed in Table 1. Plots of the derived radial distortion polynomials are shown in Figure 3.

From a comparison of the results listed in Table 1, it is possible to draw a few tentative conclusions regarding the *a posteriori* precision of the distortion coefficients and the Gaussian focal lengths. It is first notable that, whereas the distortion polynomial for an object distance of 2 m was not found to be statistically significant in the solution without constraints, in the constrained adjustment this distortion function was found to be significant at a 5 percent significance level.

At focal settings of 1.6 m and 3 m there is very little difference between the constrained and unconstrained solutions. A marginal improvement in the *a posteriori* precision of the lens distortion coefficients is apparent, but there is no change in the correlation coefficients. Estimates of the Gaussian focal length at 1.6 m and 3 m obtained in the two self-calibration solutions differ by an amount which is considerably less than the one sigma level.

However, whereas the constrained and unconstrained self-calibrations produce similar results for the 1.6 m and 3 m focal settings, there is a more substantial variation between the solutions at an object distance of 2 m. Here, the calculated values of the coefficients K_{i1} and K_{i2} obtained in the constrained adjustment display 25 to 30 percent smaller *a posteriori* standard errors than the unconstrained estimates. In addition, the correlation coefficient is reduced from a magnitude of 0.96 down to 0.88.

Because there is a coupling between radial lens distortion and Gaussian focal length, the large variation in the values of the distortion coefficients between the SELCAL and MULFOC solutions is also matched by a variation of 190 μm between the two adjusted principal distances at 2 m. To enable a direct comparison to be made between the two symmetric radial distortion polynomials determined for the 2 m focal setting, an equivalent distortion curve has been calculated by balancing the first polynomial so that the equivalent principal distance of the unconstrained solution matches the value obtained in the constrained solution. This equivalent distortion polynomal is shown in Figure 3.

Conclusions

In order to appreciate the attainable accuracy of a multiple focal setting self-calibration using the Hasselblad MK-70, one need only consider the root-mean-square (RMS) values of the image coordinate residuals, and the derived precision of the object space target point coordinates. In the self-calibration with linear constraints, RMS values of $s_x = \pm 3.3$ μm and $s_y = \pm 3.5$ μm were obtained, whereas in the constrained adjustment these values were reduced in magnitude to $s_x = \pm 3.1$ μm and $s_y = \pm 3.2$ μm. The *a posteriori* standard errors of the (X,Y,Z) coordinates for points in the midfield of the target range were of the order of $\sigma_x \simeq \sigma_y \simeq 50$ μm and $\sigma_z \simeq 90$ μm (with respect to the assigned reference coordinate system). Expressed in the form of a ratio of the standard error over the diameter of the object target field, the precision in X and Y coordinates is about 1/60,000, whereas the figure for the Z coordinate determination is approximately 1/35,000. The coordinate precision of points on the wires and points in the outfield is less than that just given; however, the poorest estimate is still on the order of 1/25,000. It is considered unlikely that such high accuracy will be achieved in similar close-range photogrammetric surveys employing a metric film camera with a lens of 60-mm focal length, unless an analytical self-calibration technique is adopted for the phototriangulation.

In conclusion, the principal advantage of the proposed multiple focal setting self-calibration technique is considered to be the fact that self-calibrated radial distortion polynomial coefficients at different principal distances, which have hitherto been treated as uncorrelated functions in the adjustment, display a linear relationship with magnification which is consistent with established theory. Even

though a long focal length camera with a pronounced distortion profile would probably have been a more appropriate camera to use in the present experimental program, the results obtained using the Hasselblad MK-70 with a Biogon 60 mm lens suggest that the proposed multiple focal setting self-calibration provides a useful one-step calibration technique for close-range metric cameras.

ACKNOWLEDGMENTS

The author gratefully acknowledges the beneficial discussions on the project held with Dr. S. A. Veress. He also wishes to thank Mr. R. M. Enoka for his useful comments on the first draft of the paper.

REFERENCES

Abdel-Aziz, Y. I., 1973. Lens Distortion and Close Range, *Photogrammetric Engineering*, Vol. 39, pp. 611-616.

Brown, D. C., 1971. Close-Range Camera Calibration, *Photogrammetric Engineering*, Vol. 37, pp. 855-866.

_____, 1972. *Calibration of Close-Range Cameras.* Invited paper, XIIth Congress of ISP, Comm. V, Ottawa.

_____, 1974. Bundle Adjustment with Strip- and Block-Invariant Parameters, *BuL*, Vol. 42, pp. 210-220.

_____, 1976. *The Bundle Adjustment-Progress and Prospects*, Invited paper Comm. III, XIIIth Congress of ISP, Helsinki.

Bunch, J. R., and B. N. Parlett, 1971. Direct Methods for Solving Symmetric Indefinite Systems of Linear Equations, *SIAM J. Numer. Anal.*, Vol. 8, No. 4, pp. 639-655.

Ebner, H., 1976. Self-Calibrating Block Adjustment, *BuL*, Vol. 44, No. 4, pp. 128-139.

El Hakim, S. F., and W. Faig, 1979. Combined Geodetic and Photogrammetric Adjustment for Densification of Control Networks, *Proc. ASP 45th Annual Meeting*, Washington, March, pp. 582-590.

Fraser, C. S., and S. A. Veress, 1979. Self-Calibration of a Fixed-Frame Multiple Camera System, submitted for publication in *Photogrammetric Engineering and Remote Sensing*. Submitted July '79 and currently under review.

Gotthardt, E., 1975. Zusatzglieder bei der Aerotriangulation mit Bündeln, *BuL*, Vol. 43, No. 6, pp. 218-221.

Grün, A., 1978. *Experiences with Self-Calibrating Bundle Adjustment*, Presented paper, ASP 44th Annual Meeting, Washington, February.

Hamilton, W. C., 1964. *Statistics in Physical Science*, The Ronald Press Company, New York, 230 pp.

Kenefick, J. F., M. S. Gyer, and W. F. Harp, 1972. Analytical Self-Calibration, *Photogrammetric Engineering*, Vol. 38, pp. 1117-1126.

Magill, A. A., 1955. Variation in Distortion with Magnification, Research paper 2574, *J. Research of the National Bureau of Standards*, Vol. 54, No. 3, pp. 135-142.

Salmenperä, H., J. M. Anderson, and A. Savolainen, 1974. Efficiency of The Extended Mathematical Model in Bundle Adjustment, *BuL*, Vol. 42, No. 6, pp. 229-233.

Schut, G., 1978. Selection of Additional Parameters for Bundle Adjustment, *Proc., ASP Fall Technical Meeting*, Albuquerque, pp. 490-503.

(Received 30 May 1979; revised and accepted 26 April 1980)

Short Course
Optical Science and Engineering

Doubletree Inn, Tucson, Arizona
12-23 January 1981

The purpose of the course is to acquaint both the specialist and the non-specialist engineer or scientist with the latest techniques in the design and engineering of optical systems. The course comprises 18 three-hour lectures; detailed notes will be supplied.

The wide range of topics that will be covered includes geometrical and physical optics, optical system layout and design, Fourier methods, digital image processing, polarized light, radiometry, image quality, interferometry and optical testing, thin films, photodetectors, and visible and infrared systems.

For further information please contact

Philip N. Slater
Optical Systems & Engineering Short Courses Inc.
P.O. Box 18667
Tucson, AZ 85731